

Elemental Mapping and Geochemical Characterization of Gas Producing Shales by Laser Induced Breakdown Spectroscopy

Jinesh Jain^{a,c}, C. Derrick Quarles Jr.^{d#}, Johnathan Moore^{b,e}, Daniel A. Hartzler^{a,c}, Dustin McIntyre^b, Dustin Crandall^b

^a DOE National Energy Technology Laboratory, Pittsburgh, PA, USA

^b DOE National Energy Technology Laboratory, Morgantown, WV, USA

^c AECOM at the National Energy Technology Laboratory, Pittsburgh, PA, USA

^d Applied Spectra, Inc, Fremont, CA, USA

^e AECOM at the National Energy Technology Laboratory, Morgantown, WV, USA

current address: Elemental Scientific, Inc., Omaha, NE, USA

Abstract

Laser induced breakdown spectroscopy (LIBS) has been used for the analysis of hydrocarbon bearing shale samples. Shale samples taken from a Marcellus gas well at depths ranging from 7498-7551 feet (2285.4 – 2301.5 m) were analyzed by LIBS using an 81 x 81 grid pattern covering an 8 x 8 mm area. The data collected from these experiments were used to construct 2D elemental maps for each sample including the hydrocarbon forming elements C and H. Results show that the spatial elemental composition of the shale varies due to the matrix of the rock, and as a function of the sample depth. The accuracy of analysis was confirmed by analyzing a shale sample of known elemental concentrations and obtaining a good agreement between analyzed and reference values. It has been shown that LIBS can be used to determine elemental composition variations in hydrocarbon bearing shales in a laboratory setting. Extending this capability into wellbores will enable producers to rapidly target resources with greater accuracy.

Keywords: Laser Induced Breakdown Spectroscopy, Elemental Analysis, Hydrocarbon, Marcellus Shale

Introduction

Natural gas production world-wide is projected to increase substantially by 2040 and shale gas is expected to account for 30% of this increase in production [1]. Therefore, it is crucial to develop techniques that are cost effective, rapid, and precise to help producers and researchers alike determine the composition of these reservoir rocks. This will not only allow well operators to determine rock properties prior to major completion activities but also help inform the hydrocarbon potential in the highly heterogeneous shale reservoirs.

The Marcellus shale formation in the eastern United States is an organic rich shale that has been a prolific producer of natural gas and is the largest reservoir of natural gas in the Appalachian basin, having an estimated reserve of 77.2 trillion cubic feet [2]. The production of hydrocarbons from unconventional shale plays has increased drastically over the last 2 decades with improvements to horizontal drilling and hydraulic fracturing techniques [3, 4]. However, characterization of reservoir rock is still a vital first step in identifying best practices and production techniques. Knowledge of elemental composition provides insight into key rock properties, such as porosity, permeability, and the presence of minerals (which can be identified using a variety of techniques [5-14]) that affect oil and gas production and influence decisions about drilling methodologies.

Currently, X-ray fluorescence (XRF) is the preferred technique for the elemental analysis of rock cores due to its low cost and fast acquisition times [15]. Scanning electron microscopy-energy dispersive spectroscopy (SEM-EDS) has also been used for the spectral mapping of shale samples for distribution analysis [16]. However, this is a more time and cost intensive analysis technique and requires careful sample preparation [17]. These techniques rely on the rock samples to be extracted from the wellbore and transported to the lab; handheld XRF surveys can be conducted in the field, but still require extraction from the wellbore. XRF is limited by poor lower

detection limits [18], particularly for light elements and is not suitable for the analysis of carbon and hydrogen [19, 20], which can indicate the presence of hydrocarbons. Also, while SEM-EDS can detect carbon, it is insensitive to hydrogen [17]. In addition to the two aforementioned techniques, destructive testing, which can also be time and cost intensive, is needed to obtain representative C and H values [21]. In this methodology, we propose laser induced breakdown spectroscopy (LIBS) as an alternative analytical technique for the simultaneous analysis of metals, light elements, and H/C values.

LIBS is a rapidly advancing and fast analytical technique for core analysis [8-10, 22-24] that requires minimal sample preparation and can theoretically provide concentrations of every element on the periodic table of a given sample [25-27]. In LIBS, a pulsed high energy laser beam is focused on the sample to be analyzed forming a plasma; characteristic spectral signatures of elements present in the sample are collected and analyzed to extract the necessary information. The technique is able to perform both surface (2D spatial) and depth analysis of a sample [28, 29]. Additionally, LIBS can operate in extreme conditions, has a high degree of flexibility in probe design and uses fiber optics which make it an attractive tool for *in-situ* analysis in harsh environments and difficult to reach places [30-36]. In-situ analysis can be useful in the situations where the results may be affected by the ambient conditions at the land surface and sample disturbance during extraction is an issue; it also reduces cost by lessening the need for difficult core recovery.

In this study, LIBS is evaluated for analysis of Marcellus shale samples taken from depth at the Marcellus Shale Energy and Environment Laboratory (MSEEL). Located in Morgantown, WV, MSEEL is a field site with multiple production and scientific wells sponsored by the Department of Energy (DOE) National Energy Technology Laboratory (NETL) and operated by

West Virginia University, Northeast Natural Energy, Ohio State University, Schlumberger, and other partners (www.MSEEL.org [37]). MSEEL is a highly instrumented and transparent well that has given researchers access to highly coveted well data and provided a platform for demonstration of some of the most advanced techniques to-date being employed in tight shale gas production. Ongoing research at MSEEL is evaluating long-term environmental impacts and improvement of production techniques based on data gathered at the site.

2. Material and Methods

2.1 Sample and preparation

The MSEEL shale samples used in this study were taken from a Marcellus gas well (MIP 3H) at depths ranging from 7498-7551 feet (2285.4 – 2301.5 m). The composition of the Marcellus is highly variable across the basin, and has been reported in previous studies to be composed of 9-35% mixed-layer clays, 10-60% quartz, 0-10% feldspar, 5-13% pyrite, 3-48% calcite, 0-10% dolomite, and 0-6% gypsum [2, 38-42]. The organic content is variable as well, ranging from 1 – 20% [2], but typically on the lower half of this range. Shale samples were cut into pieces that ranged from 20 – 60 mm laterally and < 10 mm in thickness. Calibration curves were prepared from ICP-OES data taken from Marcellus shale outcrop samples, a gray shale from Petersburg WV and a black shale from Bedford PA [43-45]. These outcrop samples were also analyzed for C and H content at the University of Western Kentucky using the Leco CHN TrueSpec and ASTM method D 5373 and ranged in C and H content from 1.23 – 9.33 wt. % and 0.50 – 0.54 wt. %, respectively. The MSEEL core had been previously characterized by handheld XRF at 16.7 mm intervals and the total organic carbon (TOC) was measured by pyrolysis at three-foot (change to exact number) intervals. XRF data was measured on the core surface by an Innov-X® Delta

Standard M-6000 X-Ray Fluorescence Spectrometer for 120s per beam using the dual beam mining mode [46]. Pyrolysis data was measured by a Weatherford Source Rock Analyzer.

2.2 Instrumentation

Samples were analyzed using a J200 LIBS instrument (Applied Spectra, Inc., Fremont, CA). The J200 instrument is equipped with a 266 nm, 8 ns Nd:YAG laser, a 6 channel CCD broadband spectrometer with a spectral window of 185 – 1050 nm, and a gas purged sample chamber. The system is fully integrated and controlled using Applied Spectra's Axiom® operation software. The method conditions are listed in Table 1 for both the calibration and mapping methods. Ultra-high purity helium gas (Praxair Inc., San Jose, CA) was used for all experiments to purge the sample chamber of any atmospheric gases. All data (spectra, calibration curves, and elemental maps) were analyzed using Applied Spectra's Data Analysis package. Each data point in the elemental maps is the integral of an elemental peak from the spectrum.

Table 1. LIBS conditions for the shale maps and calibration samples.

	Shale Maps	Calibration Samples
<i>Laser spot size</i>	50 μm	50 μm
<i>Laser energy</i>	6.75 mJ	6.75 mJ
<i>Laser repetition rate</i>	10 Hz	10 Hz
<i>Gas environment</i>	0.5 L/min He	0.5 L/min He
<i>Spectrometer delay</i>	0.25 μs	0.25 μs
<i>Laser pulses</i>	5 pulses per location	5 pulses per location
<i>Analyzed area</i>	8 mm x 8 mm (64 mm ²)	8 mm x 8 mm (64 mm ²)
<i>Mapping method type</i>	Grid points	Grid points
<i>Mapping method size</i>	81 x 81 (6,561 data points)	5 x 5 (25 data points)
<i>Time per sample</i>	390 min	1 min 32 sec

3. Results and Discussions

Four Marcellus samples retrieved from depths 7498' (2285.4 m), 7504' (2287.2 m), 7531' (2295.4 m), and 7551' (2301.5 m) were analyzed to assess LIBS in comparison with traditional techniques and are identified as M7498, M7504, M7531, and M7551, respectively. The images

indicating the size of shale specimens and their corresponding depth is presented in Figure 1. An 81 x 81 grid that covered an 8 mm x 8 mm (64 mm²) area was used for LIBS scanning. Several elements including Al, C, Ca, Fe, H, Mg, O, and Si were mapped for this study, although this is not a complete list of the elements detected. It should be noted that all mapping was done along the shale bedding plane surfaces. Samples were not polished beforehand, however, the instrument's autofocus capability is able to compensate for the uneven sample surface. To avoid any absorption of C and H from the air, all samples were kept under a helium environment for about 30 minutes prior to and during the analysis.. The comparison of the 1st laser shot with shots 2-5 did not reveal any evidence of sample surface contamination (data not shown).

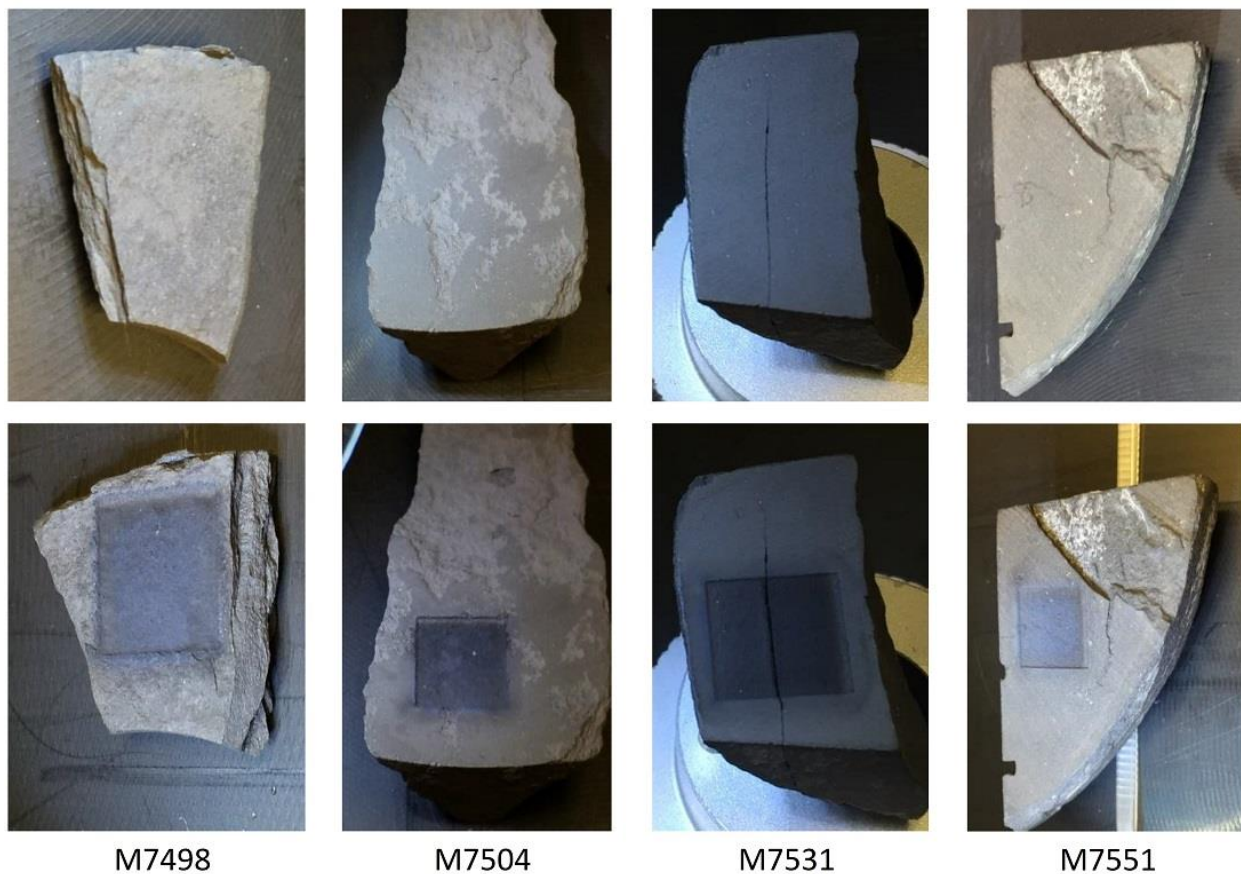


Figure 1: Images of the shale samples before and after ablation. Four Marcellus shales (M7531, M7551, M7504, and M7498) were included in this study. Samples were mapped along the bedding plane surfaces.

The data collected for these elements were used to construct 2D maps for each shale sample. Each spectrum utilized 5 laser shots per location to provide a good signal-to-noise ratio. A representative map for Al is presented in Figure 2. In this case the 394.37 nm plasma emission line of Al was used to generate a 2D image using the x-y coordinates of the ablated area.

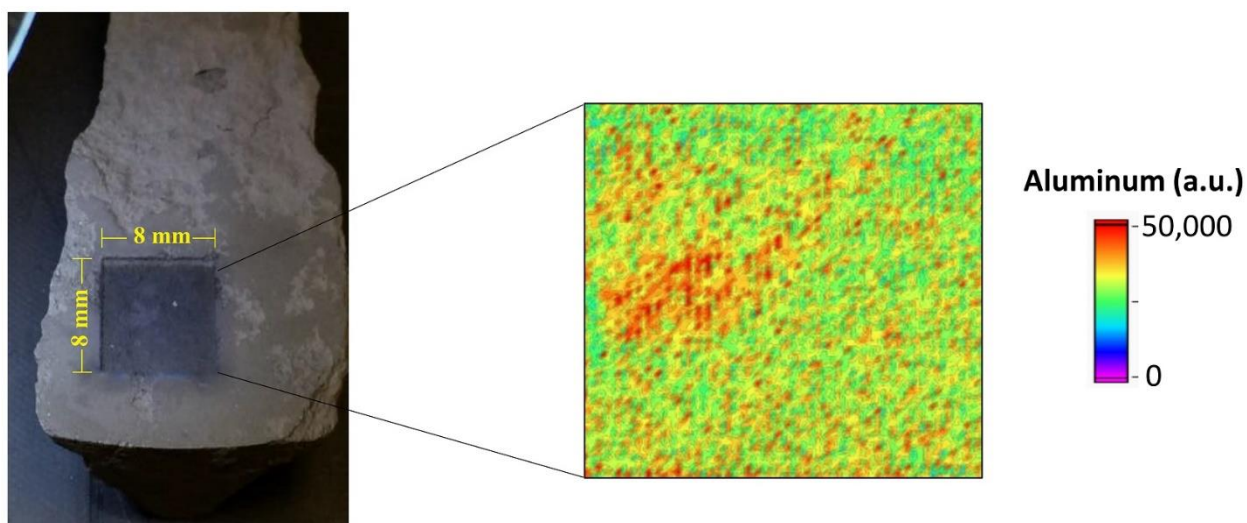


Figure 2. Image of the ablated area and the Al 394.37 nm emission intensity map created from the LIBS measurements of the M7504 sample.

Figure 3 displays the uncalibrated emission intensity maps for Ca, Al, O, Fe, Mg, and Si of the shale samples. Simple visual comparison illustrates the heterogeneity inherent to the samples, which is expected of natural materials. Within the mapped area of each sample a heterogeneous distribution for most of the elements is evident (Figure 3).

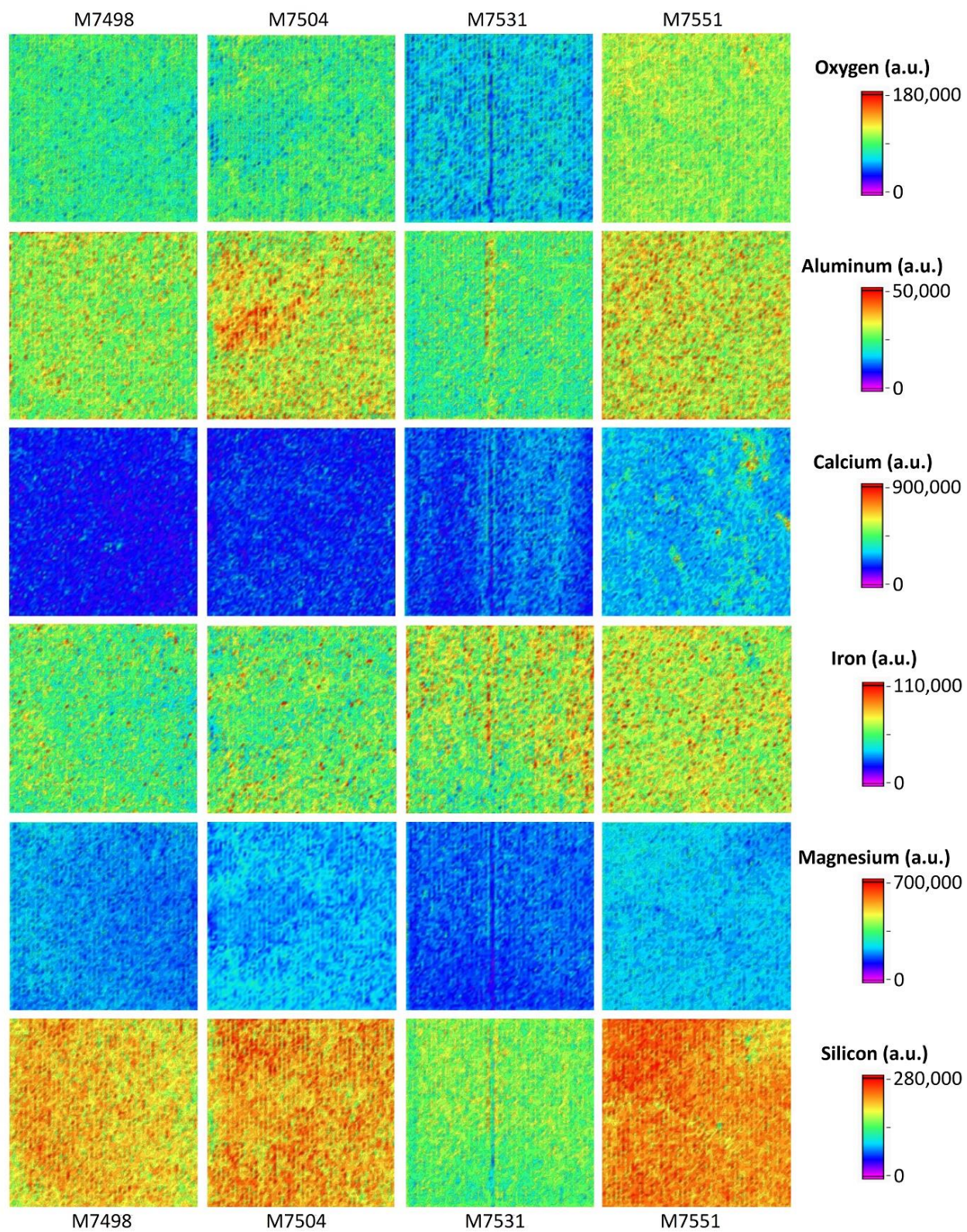


Figure 3. Intensity maps of O 777.30 nm, Al 394.37 nm, Ca 393.36 nm, Fe 274.80 nm, Mg 280.27 nm, and Si 288.16 nm for the 4 shale samples. Since the plasma emission

intensity differs for each element, the data sets were normalized by max intensity per element to facilitate visual comparison of these different components. Extra Al and Fe counts seen in the region of the crack in sample M7551 are an artifact likely caused by the laser and collection optics being out of focus when passing over the crack.

Because of its excellent detection limits and capability of analyzing lighter elements, LIBS is a suitable technique for determination of C and H. For analysis of hydrogen the most intense and interference free atomic line H 656.29 nm was used. The 247.86 nm carbon line is susceptible to interferences by major elements present in shale (specifically Fe, [47]) therefore, the C 193.09 nm atomic line was chosen for analysis of carbon. A comparison of maps for the two carbon lines confirms that the most intense C 247.86 nm line suffers from interferences however, the second most intense line C 193.09 nm was free of interferences and can be used to generate meaningful data. Figure 4 shows the uncalibrated C and H emission intensity maps organized by increasing depth from where the shale samples were retrieved, and a visual comparison shows that sample M7504 has relatively higher C and H contents compared to the other samples, further demonstrating the heterogeneity of the Marcellus shale.

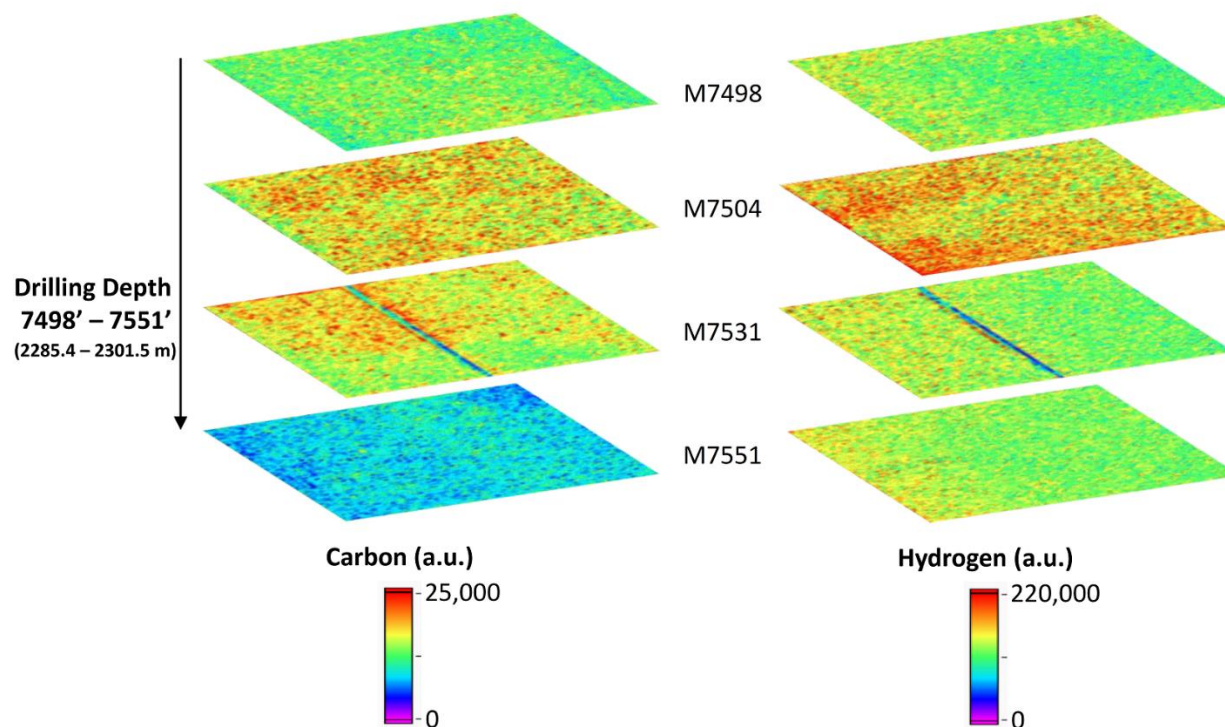


Figure 4. Intensity maps of C 193.09 nm and H 656.29 nm for the 4 shale samples based on drilling depth.

LIBS requires calibration in order to quantify the collected data. To our knowledge matrix matched calibration standards (i.e. physically and chemically identical samples of known concentration) for shale are not available commercially. Therefore, Marcellus shale outcrop samples characterized by ICP-OES and CHN analysis were utilized as calibration standards. The outcrop samples were mapped along with the unknown Marcellus shale samples to create calibration curves for all the elements. Calibration curves for C and H are presented in Figure 5. The C 193.09 nm line was used for calibrating carbon while hydrogen was calibrated using the atomic line H 656.29 nm, both lines lack interferences that would affect the response. The calibration curves for both C and H show good linearity with correlation coefficients (R^2) of 0.9954 and 0.9933, respectively. It must be noted that, while the outcrop shale samples appear to be a

matrix matched calibration standards, multiple sources of uncertainty exist to compromise the quantification of the analysis. Geological samples often contain multiple phases (e.g. quartz, calcite, etc.) each with their own local matrix to make it difficult to truly match the sample matrix to the standards and blanks. As indicated in the literature () some of these factors may prevent passing of calibration curve through the origin. Therefore, a rigorous quantitative measurement are needed to to account for the matrix effects of each phase encountered. A number of data analysis techniques available in the literature can provide detailed information about the samples such as the type and distribution of mineral or organic phases [8-13],.

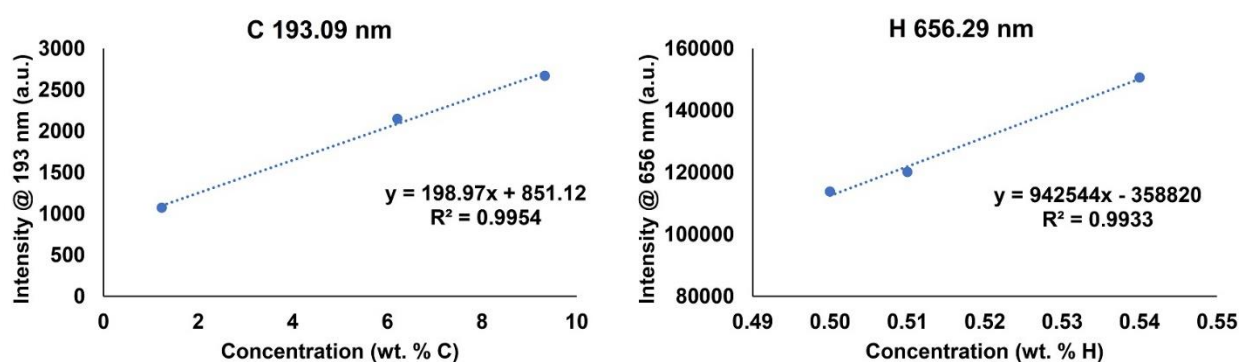


Figure 5. Calibration curves for C 193.09 nm and H 656.29 nm based on 5 x 5 ablated grid.

Using these calibration curves, the emission intensity maps for C and H (Figure 4) were converted to concentration maps (Figure 6). It is clear from the figure that C and H concentrations vary dramatically from sample to sample. Average concentrations of C and H for all 4 samples are presented in Table 2, which ranged from ~ 5.89 – 9.26 wt. % carbon and ~ 0.46 – 0.53 wt. % hydrogen. Like in the qualitative maps (Figure 4), the MSEEL sample (M7504) shows the highest concentration of both C and H, with average concentrations of 9.26% and 0.53% respectively. These concentrations are the highest among all the samples and support the observations made in the concentration maps in Figure 6. Based on these calibration standards the limits of detection for

C 193 nm and H 656 nm were calculated to be 848 ppm and 3.5 ppm, respectively. The limits of detection were calculated as $3\sigma/m$ where σ is the standard deviation of the background around the peak and m is the slope of the calibration curve [48].

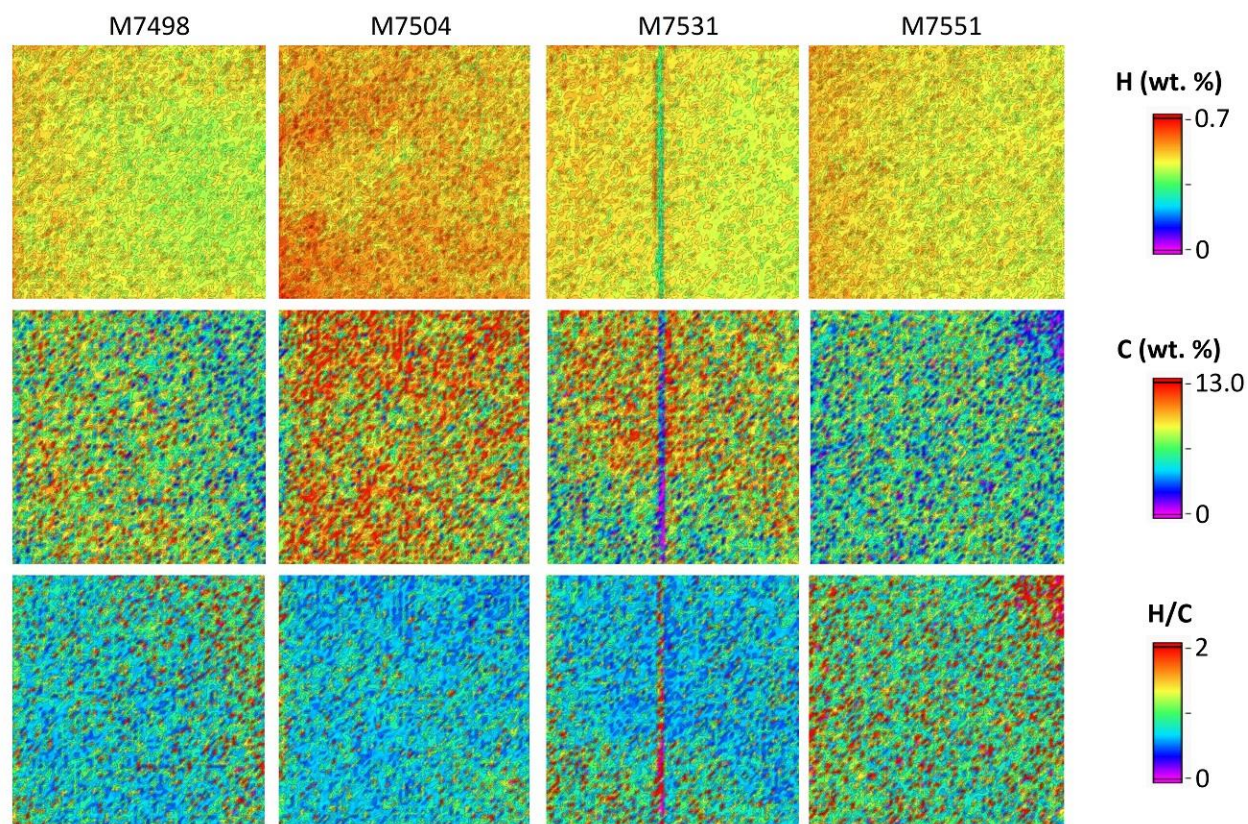


Figure 6. Concentration maps of C and H determined for each of the shale samples. H/C ratio maps, bottom row, were constructed using $(\text{H wt. \%}/1.00011)/(\text{C wt. \%}/12.011)$.

Table 2. Average concentration of C and H determined over the 8 x 8 mm area ($n = 6,561$ points) of each shale sample (Wt. %). RSD = relative standard deviation

	C 193	%RSD	H 656	%RSD
M7498	7.13	8.4	0.46	8.1
M7504	9.26	5.1	0.53	9.2
M7531	7.93t	8.1	0.47	9.4
M7551	5.89	21.0	0.48	7.3

Similarly, the intensity maps for other elements were converted to concentration maps (not shown) and the elements were quantified using the outcrop calibration standards. Table 3 presents the concentrations of Al, Ca, Fe, Mg, and Si averaged over each 8 mm x 8 mm area, with standard deviation (SD) for all 4 shale samples. The SD in this case gives a measure of sample heterogeneity rather than error of the scanned area in terms of mineral composition. Mapping of shale samples for major elements can not only provide information about the distribution of these elements within the shale rock but can also be used to identify the type of minerals [8-14]: e.g., silicates, aluminosilicates, carbonates, sulfides, clays, quartz, feldspar, dolomite and more.

Table 3. Average elemental concentration determined over the 8 x 8 mm area (n = 6,561 points) of each shale sample. Oxygen was not quantified due to lack of reference values.

Concentration Average Value (Wt. % \pm 1 SD)					
Sample	Al	Ca	Fe	Mg	Si
M7498	0.71 \pm 0.52	1.22 \pm 0.20	1.74 \pm 0.11	0.65 \pm 0.04	21.7 \pm 0.99
M7504	1.63 \pm 0.75	1.53 \pm 0.19	1.82 \pm 0.11	0.68 \pm 0.03	22.6 \pm 1.06
M7531	0.8 \pm 0.29	2.12 \pm 0.50	1.99 \pm 0.19	0.58 \pm 0.04	17.3 \pm 1.05
M7551	1.67 \pm 0.62	3.32 \pm 0.48	2.06 \pm 0.9	0.70 \pm 0.03	23.6 \pm 1.05

The method accuracy of the LIBS analysis is presented in Tables 4 and 5. The CHN analyzer and LIBS data (Table 4) for sample M7504 show a good agreement in both C and H values. On the other hand, the XRF and LIBS values for Al and Fe exhibit a relatively larger difference. It needs to be pointed out that the XRF analysis was performed across the bedding planes on the surface of the extracted core while the LIBS measurement was performed along the bedding planes on a core fragment. The variations in XRF and LIBS values may be because of the exact location of the analysis was different for both measurements and the shale is heterogeneous in nature (see Figures 3 and 7). Note that the Mg concentration in these samples was somehow not detected by the handheld XRF in the employed experimental conditions. Therefore, the select samples were sent

to Hamilton College Analytical Laboratory for analysis by a laboratory scale XRF spectrometer (Thermo ARL Perform'X). The reported Mg concentrations for the M7498, M7504, and M7531 samples were 0.73, 0.72, and 0.57 wt% respectively, closely matching the LIBS measured values in Table 3.

Table 4. Comparison between CHN Analysis and LIBS for the M7504 Marcellus shale sample (Wt. %).

Sample		C	H
<i>M7504</i>	CHN	9.33	0.51
	LIBS	9.26	0.53

Table 5. Comparison between handheld XRF and LIBS concentrations for shale samples (Wt. % \pm 1 SD). Note that the XRF data were collected across the shale bedding planes on the surface of the extracted core while the LIBS data were collected along the bedding planes on a core fragment.

Sample		Al	Ca	Fe	Si
<i>M7498</i>	XRF	5.18 \pm 0.13	1.60 \pm 0.01	3.85 \pm 0.03	21.27 \pm 0.12
	LIBS	0.71 \pm 0.52	1.22 \pm 0.20	1.74 \pm 0.11	21.7 \pm 0.99
<i>M7504</i>	XRF	3.39 \pm 0.97	1.48 \pm 0.01	2.75 \pm 0.02	22.1 \pm 0.11
	LIBS	1.63 \pm 0.75	1.53 \pm 0.19	1.82 \pm 0.11	22.6 \pm 1.06
<i>M7531</i>	XRF	2.16 \pm 0.11	0.84 \pm 0.01	3.21 \pm 0.03	15.44 \pm 0.11
	LIBS	0.8 \pm 0.29	2.12 \pm 0.50	1.99 \pm 0.19	17.3 \pm 1.05
<i>M7551</i>	XRF	2.13 \pm 0.09	3.21 \pm 0.02	3.55 \pm 0.03	21.72 \pm 0.12
	LIBS	1.67 \pm 0.62	3.32 \pm 0.48	2.06 \pm 0.90	23.6 \pm 1.05

The higher concentration of C and H in shale samples could be correlated to higher organic material and therefore a high gas production potential. However, understanding the type of hydrocarbons associated with the shale samples requires a quantitative analysis. While the major elements ratios can provide information about mineralogy of the shale, the H/C ratios can give an indication of the type of hydrocarbons present in the sample. Since shale gas is primarily composed of methane, the H/C ratios can potentially be used to predict the type of hydrocarbons and impurities in the shale gas deposits. The concentration data presented in Table 2 and Figure 6 were

converted to H/C ratios using the following equation: $H/C \text{ ratio} = (H\%/1.00011)/(C\%/12.011)$. Table 6 portrays the average H/C values determined for each shale sample, the ratios vary between 0.76 and 1.05 for all the shale samples. If the C and H contents solely represent the organic compounds, the H/C ratio can predict the nature of hydrocarbons and the quality of the gas in shale deposits. In fact, shale deposits rich in natural gas are expected to show the H/C ratio greater than 1. It should be noted that LIBS analyzes the total hydrogen and total carbon contents in a sample and doesn't discriminate between the inorganic and organic compounds. While the presence of carbonates or any other inorganic carbon compounds (e.g. CO₂) can enhance the carbon concentration the presence of moisture and hydroxyl groups can enhance the hydrogen concentration. A comparison of the total organic carbon (TOC, analyzed by pyrolysis) to total carbon (TC, analyzed by LIBS) are presented in Table 7. This data indicates a possible predictive relation between the quantities, with higher TC correlating with higher TOC, while the TOC/TC ratio indicates 30-40% of the TC is inorganic. More work is needed to see if this correlation holds true for shales from different basins or even within the same basin. Nevertheless, a simultaneous determination of the major elements as well as C and H by LIBS complements the existing techniques used in the shale industry and can potentially provide useful information favorable to oil and gas exploration. It will be worth mentioning here that LIBS has been used to estimate the heating value of oil shale and coal based on correlations between C, H, and major rock forming elements [49, 50].

Table 6. Average H/C ratio determined over the 8 x 8 mm area (n = 6,561 points) of each shale sample.

Sample	H/C
M7498	0.85
M7504	0.76
M7531	0.84
M7551	1.05

Table 7. Average total carbon (TC) from LIBS versus total organic carbon (TOC) from pyrolysis for Marcellus shale core samples (Wt. %).

Sample	TC	TOC	TOC/TC
<i>M7498</i>	7.13	4.78	0.67
<i>M7504</i>	9.26	5.92	0.64

This study shows the applicability of LIBS for shale research, and that the development of a field deployable LIBS instrument can be useful for in situ analysis of shale without retrieving the sample for laboratory analysis. Currently our laboratory is developing a fiber coupled, all optical downhole LIBS sensor based on a passively Q-switched laser [34-36, 51, 52]. As mapping techniques advance, the time required to measure large areas is dropping dramatically [8, 53] potentially allowing mapping to be used for rapid online sample analysis. The ability of LIBS to detect all elements (including C and H) and capability of downhole measurements could potentially offer a distinct advantage over existing techniques used in shale gas exploration.

Conclusions:

Spectral mapping by LIBS offers a valuable tool for distribution analysis and elemental composition of shale samples. The technique complements existing techniques used in the shale gas exploration and provides reliable and accurate data with reasonable detection limits for most of the elements including C and H. While the presence of C and H can provide a preliminary indication of the natural gas rich areas the major element concentrations can be helpful in determining the mineralogy of those areas. Shale gas is primarily composed of methane and H/C ratios can potentially predict the type of hydrocarbons and impurities in shale gas deposits. This study shows how the spatial elemental (including C and H) composition varies as a function of the sample location and illustrates the benefits of LIBS over existing analytical techniques.

Acknowledgment

This technical effort was performed in support of the National Energy Technology Laboratory's ongoing research under the RES contract DE-FE0004000.

Disclaimer

This project was funded by the Department of Energy, National Energy Technology Laboratory, an agency of the United States Government, through a support contract with AECOM. Neither the United States Government nor any agency thereof, nor any of their employees, nor AECOM, nor any of their employees, makes any warranty, expressed or implied, or assumes any legal liability or responsibility for the accuracy, completeness, or usefulness of any information, apparatus, product, or process disclosed, or represents that its use would not infringe privately owned rights. Reference herein to any specific commercial product, process, or service by trade name, trademark, manufacturer, or otherwise, does not necessarily constitute or imply its endorsement, recommendation, or favoring by the United States Government or any agency thereof. The views and opinions of authors expressed herein ***do not necessarily state or reflect those of the United States Government or any agency thereof.***

References

- [1] J. Conti, P. Holtberg, J. Diefenderfer, A. LaRose, J.T. Turnure, L. Westfall, International Energy Outlook 2016 With Projections to 2040, in, USDOE Energy Information Administration (EIA), Washington, DC (United States). Office of Energy Analysis, 2016.
- [2] O. Popova, Marcellus Shale Play Geology review, in, Energy Information Administration, 2017.
- [3] J.D. Arthur, B. Bohm, M. Layne, Hydraulic fracturing considerations for natural gas wells of the Marcellus Shale, (2009).
- [4] D.M. Kargbo, R.G. Wilhelm, D.J. Campbell, Natural gas plays in the Marcellus Shale: Challenges and potential opportunities, in, ACS Publications, 2010.
- [5] D.M. Díaz Pace, N.A. Gabriele, M. Garcimuño, C.A. D'Angelo, G. Bertucelli, D. Bertucelli, Analysis of minerals and rocks by laser-induced breakdown spectroscopy, Spectroscopy Letters, 44 (2011) 399-411.

- [6] N.J. McMillan, R.S. Harmon, F.C. De Lucia, A.M. Miziolek, Laser-induced breakdown spectroscopy analysis of minerals: carbonates and silicates, *Spectrochimica Acta Part B: Atomic Spectroscopy*, 62 (2007) 1528-1536.
- [7] Nina L. Lanza, Roger C. Wiens, Samuel M. Clegg, Ann M. Ollila, Seth D. Humphries, Horton E. Newsom, James E. Barefield, Calibrating the ChemCam laser-induced breakdown spectroscopy instrument for carbonate minerals on Mars, *Applied Optics*, 49 (2010) C211-C217.
- [8] C. Fabre, D. Devismes, S. Moncayo, F. Pelascini, F. Trichard, A. Lecomte, B. Bousquet, J. Cauzid, V. Motto-Ros, Elemental imaging by laser-induced breakdown spectroscopy for the geological characterization of minerals, *Journal of Analytical Atomic Spectrometry*, 33 (2018) 1345-1353.
- [9] F. Trichard, S. Moncayo, D. Devismes, F. Pelascini, J. Maurelli, A. Feugier, C. Sasseville, F. Surma, V. Motto-Ros, Evaluation of a compact VUV spectrometer for elemental imaging by laser-induced breakdown spectroscopy: application to mine core characterization, *Journal of Analytical Atomic Spectrometry*, 32 (2017) 1527-1534.
- [10] O. Haavisto, T. Kauppinen, H. Häkkänen, Laser-induced breakdown spectroscopy for rapid elemental analysis of drillcore, *IFAC Proceedings Volumes*, 46 (2013) 87-91.
- [11] X. Wang, V. Motto-Ros, G. Panczer, D. De Ligny, J. Yu, J.-M. Benoit, J.-L. Dussossoy, S. Peugeot, Mapping of rare earth elements in nuclear waste glass-ceramic using micro laser-induced breakdown spectroscopy, *Spectrochimica Acta Part B: Atomic Spectroscopy*, 87 (2013) 139-146.
- [12] S. Pagnotta, M. Lezzerini, B. Campanella, G. Gallelo, E. Grifoni, S. Legnaioli, G. Lorenzetti, F. Poggialini, S. Raneri, A. Safi, Fast quantitative elemental mapping of highly inhomogeneous materials by micro-Laser-Induced Breakdown Spectroscopy, *Spectrochimica Acta Part B: Atomic Spectroscopy*, 146 (2018) 9-15.
- [13] J. Klus, P. Pořízka, D. Prochazka, P. Mikysek, J. Novotný, K. Novotný, M. Slobodník, J. Kaiser, Application of self-organizing maps to the study of U-Zr-Ti-Nb distribution in sandstone-hosted uranium ores, *Spectrochimica Acta Part B: Atomic Spectroscopy*, 131 (2017) 66-73.
- [14] G.S. Senesi, Laser-Induced Breakdown Spectroscopy (LIBS) applied to terrestrial and extraterrestrial analogue geomaterials with emphasis to minerals and rocks, *Earth-Science Reviews*, 139 (2014) 231-267.
- [15] B. Scraggs, M. Haschke, L. Herczeg, J. Nicolosi, XRF mapping: new tools for distribution analysis, *Advances in X-ray Analysis*, 42 (2000) 19-25.
- [16] H. Aljamaan, C.M. Ross, A.R. Kovscek, Multiscale imaging of gas adsorption in shales, in: *SPE Unconventional Resources Conference*, Society of Petroleum Engineers, 2017.
- [17] D.E. Newbury, N.W. Ritchie, Performing elemental microanalysis with high accuracy and high precision by scanning electron microscopy/silicon drift detector energy-dispersive X-ray spectrometry (SEM/SDD-EDS), *Journal of materials science*, 50 (2015) 493-518.
- [18] P. Farkov, L. Il'icheva, A. Finkel'shtein, X-ray fluorescence determination of carbon, nitrogen, and oxygen in fish and plant samples, *Journal of Analytical Chemistry*, 60 (2005) 426-430.
- [19] L. Löwemark, H.-F. Chen, T.-N. Yang, M. Kylander, E.-F. Yu, Y.-W. Hsu, T.-Q. Lee, S.-R. Song, S. Jarvis, Normalizing XRF-scanner data: a cautionary note on the interpretation of high-resolution records from organic-rich lakes, *Journal of Asian Earth Sciences*, 40 (2011) 1250-1256.
- [20] A. Migliori, P. Bonanni, L. Carraresi, N. Grassi, P. Mando, A novel portable XRF spectrometer with range of detection extended to low-Z elements, *X-Ray Spectrometry*, 40 (2011) 107-112.
- [21] R. Nadkarni, Analytical techniques for characterization of oil shales, *Am. Chem. Soc., Div. Pet. Chem., Prepr.;*(United States), 28 (1983).
- [22] T. Xu, J. Liu, Q. Shi, Y. He, G. Niu, Y. Duan, Multi-elemental surface mapping and analysis of carbonaceous shale by laser-induced breakdown spectroscopy, *Spectrochimica Acta Part B: Atomic Spectroscopy*, 115 (2016) 31-39.
- [23] L. Streubel, L. Jacobsen, S. Merk, M. Thees, D. Rammlmair, J. Meima, D. Mory, Rapid Analysis of Geological Drill-Cores with LIBS, *Optik & Photonik*, 11 (2016) 23-27.

- [24] K. Kuhn, J.A. Meima, D. Rammlmair, C. Ohlendorf, Chemical mapping of mine waste drill cores with laser-induced breakdown spectroscopy (LIBS) and energy dispersive X-ray fluorescence (EDXRF) for mineral resource exploration, *Journal of Geochemical Exploration*, 161 (2016) 72-84.
- [25] A.J.R. Bauer, S.G. Buckley, Novel Applications of Laser-Induced Breakdown Spectroscopy, *Applied spectroscopy*, 71 (2017) 553-566.
- [26] F. Anabitarte, A. Cobo, J.M. Lopez-Higuera, Laser-induced breakdown spectroscopy: fundamentals, applications, and challenges, *ISRN Spectroscopy*, 2012 (2012).
- [27] R.S. Harmon, R.E. Russo, R.R. Hark, Applications of laser-induced breakdown spectroscopy for geochemical and environmental analysis: A comprehensive review, *Spectrochimica Acta Part B: Atomic Spectroscopy*, 87 (2013) 11-26.
- [28] J.R. Chirinos, D.D. Oropeza, J.J. Gonzalez, H. Hou, M. Morey, V. Zorba, R.E. Russo, Simultaneous 3-dimensional elemental imaging with LIBS and LA-ICP-MS, *Journal of Analytical Atomic Spectrometry*, 29 (2014) 1292-1298.
- [29] H. Hou, L. Cheng, T. Richardson, G. Chen, M. Doeff, R. Zheng, R. Russo, V. Zorba, Three-dimensional elemental imaging of Li-ion solid-state electrolytes using fs-laser induced breakdown spectroscopy (LIBS), *Journal of Analytical Atomic Spectrometry*, 30 (2015) 2295-2302.
- [30] A. Whitehouse, J. Young, I. Botheroyd, S. Lawson, C. Evans, J. Wright, Remote material analysis of nuclear power station steam generator tubes by laser-induced breakdown spectroscopy, *Spectrochimica Acta Part B: Atomic Spectroscopy*, 56 (2001) 821-830.
- [31] M. López-Claros, F.J. Fortes, J.J. Laserna, Subsea spectral identification of shipwreck objects using laser-induced breakdown spectroscopy and linear discriminant analysis, *Journal of Cultural Heritage*, (2017).
- [32] B. Thornton, T. Takahashi, T. Sato, T. Sakka, A. Tamura, A. Matsumoto, T. Nozaki, T. Ohki, K. Ohki, Development of a deep-sea laser-induced breakdown spectrometer for in situ multi-element chemical analysis, *Deep Sea Research Part I: Oceanographic Research Papers*, 95 (2015) 20-36.
- [33] R.C. Wiens, S. Maurice, B. Barraclough, M. Saccoccio, W.C. Barkley, J.F. Bell, S. Bender, J. Bernardin, D. Blaney, J. Blank, The ChemCam instrument suite on the Mars Science Laboratory (MSL) rover: Body unit and combined system tests, *Space Science Reviews*, 170 (2012) 167-227.
- [34] C.G. Carson, C. Goueguel, J. Jain, D. McIntyre, Development of laser-induced breakdown spectroscopy sensor to assess groundwater quality impacts resulting from geologic carbon sequestration, in: *Micro-and Nanotechnology Sensors, Systems, and Applications VII*, International Society for Optics and Photonics, 2015, pp. 94671K.
- [35] C. Goueguel, D.L. McIntyre, J.P. Singh, J. Jain, A.K. Karamalidis, Laser-induced breakdown spectroscopy (LIBS) of a high-pressure CO₂-water mixture: Application to carbon sequestration, *Applied spectroscopy*, 68 (2014) 997-1003.
- [36] C.L. Goueguel, J.C. Jain, D.L. McIntyre, C.G. Carson, H.M. Edenborn, In situ measurements of calcium carbonate dissolution under rising CO₂ pressure using underwater laser-induced breakdown spectroscopy, *Journal of Analytical Atomic Spectrometry*, 31 (2016) 1374-1380.
- [37] T.R. Carr, T.H. Wilson, P. Kavousi, S. Amini, S. Sharma, J. Hewitt, I. Costello, B. Carney, E. Jordon, M. Yates, Insights from the Marcellus Shale Energy and Environment Laboratory (MSEEL), in, *Unconventional Resources Technology Conference (URTEC)*, 2017.
- [38] M.L. Boyce, T.R. Carr, Lithostratigraphy and petrophysics of the Devonian Marcellus interval in West Virginia and southwestern Pennsylvania, T. Carr, (2009) 254-281.
- [39] J.B. Roen, Geology of the Devonian black shales of the Appalachian Basin, *Organic Geochemistry*, 5 (1984) 241-254.
- [40] R.E. Zielinski, R.D. McIver, Resource and exploration assessment of the oil and gas potential in the Devonian gas shales of the Appalachian Basin, in, *Monsanto Research Corp., Miamisburg, OH (USA). Mound*, 1981.

- [41] G. Wrightstone, Marcellus Shale: Regional overview from an industry perspective (abs.), in, AAPG Eastern Section Meeting, 2008.
- [42] K. Avary, J. Lewis, New Interest in Cores Taken Thirty Years Ago: The Devonian Marcellus Shale in Northern West Virginia, in, AAPG Eastern Section Meeting, 2008.
- [43] L. Hong, J. Jain, V. Romanov, C. Lopano, C. Disenhof, A. Goodman, S. Hedges, D. Soeder, S. Sanguinito, R. Dilmore, An investigation of factors affecting the interaction of CO₂ and CH₄ on shale in Appalachian Basin, *Journal of Unconventional Oil and Gas Resources*, 14 (2016) 99-112.
- [44] H.K. Sanghavi, J. Jain, A. Bol'shakov, C. Lopano, D. McIntyre, R. Russo, Determination of elemental composition of shale rocks by laser induced breakdown spectroscopy, *Spectrochimica Acta Part B: Atomic Spectroscopy*, 122 (2016) 9-14.
- [45] C.W. Noack, J.C. Jain, J. Stegmeier, J.A. Hakala, A.K. Karamalidis, Rare earth element geochemistry of outcrop and core samples from the Marcellus Shale, *Geochemical transactions*, 16 (2015) 6.
- [46] T.J. Paronish, Meso- and Macro-Scale Facies and Chemostratigraphic Analysis of Middle Devonian Marcellus Shale in Northern West Virginia, USA, in: Department of Geology and Geography, West Virginia University, 2018, pp. 94.
- [47] A. Kramida, K. Olsen, Y. Ralchenko, NIST LIBS Database in, National Institute of Standards and Tehcnology, pml.nist.gov/libs.
- [48] J. El Haddad, L. Canioni, B. Bousquet, Good practices in LIBS analysis: Review and advices, *Spectrochimica Acta Part B: Atomic Spectroscopy*, 101 (2014) 171-182.
- [49] M. Aints, P. Paris, M. Laan, K. Piip, H. Riisalu, I. Tufail, Determination of Heating Value of Estonian Oil Shale by Laser-Induced Breakdown Spectroscopy, *Journal of Spectroscopy*, 2018 (2018).
- [50] C.E. Romero, R. De Saro, LIBS analysis for coal, in: *Laser-Induced Breakdown Spectroscopy*, Springer, 2014, pp. 511-529.
- [51] J.C. Jain, C.L. Goueguel, D. McIntyre, Development of LIBS Sensor for Sub-Surface CO₂ Leak Detection in Carbon Sequestration, in: AIChE Annual Meeting, Minneapolis, MN, 2017.
- [52] D.H. Hartzler, J.C. Jain, D.L. McIntyre, Prototype LIBS Sensor for Sub-Surface Water Quality Monitoring with Applications in Carbon Storage, in: AIChE Annual Meeting, Pittsburgh, PA, 2018.
- [53] J. Cáceres, F. Pelascini, V. Motto-Ros, S. Moncayo, F. Trichard, G. Panczer, A. Marín-Roldán, J. Cruz, I. Coronado, J. Martín-Chivelet, Megapixel multi-elemental imaging by Laser-Induced Breakdown Spectroscopy, a technology with considerable potential for paleoclimate studies, *Scientific reports*, 7 (2017) 5080.